Semiconductor Photocatalysis.[1] ZnS-Catalyzed Photoreduction of Aldehydes and Related Derivatives: Two-Electron-Transfer Reduction and Relationship with Spectroscopic Properties

Shozo Yanagida,* Yoshiteru Ishimaru, Yoshio Miyake, Tsutomu Shiragami, Chyongjin Pac,

Chemical Process Engineering, Faculty of Engineering, Osaka University, Suita, Osaka 565, Japan

Kazuhito Hashimoto, and Tadayoshi Sakata*

Institute for Molecular Science, Myodaiji, Okazaki 444, Japan *(Received: July 5, 1988; In Final Form: September 7, 1988)*

Photocatalytic activity and spectroscopic properties of ZnS suspensions for the two-electron reduction of aldehydes or related compounds in aqueous medium are described. The ZnS suspension (ZnS-0) prepared by cooling from aqueous $ZnSO_4$ and Na_2S solutions catalyzes photoredox reactions of acetaldehyde, giving ethanol without much H_2 evolution as a two-electron-reduction product, and acetic acid, biacetyl, and acetoin as oxidation products. When the ZnS-0 suspension is refluxed (giving ZnS-100) or dried to powder, the resulting ZnS shows an increased activity for H_2 evolution but a decreased activity for the two-electron reduction. The two-electron photoreduction is ascribed to the sequential transfer of active electrons in the conduction band of defect-free aggregates of ZnS microcrystallites (quantized ZnS). This mechanism is supported by product analysis, energetics at ZnS interfaces, the sharp and blue-shifted onset of absorption and excitation spectra, and the long-life band gap emission of the active ZnS-0 suspension. UV, emission, and ESR spectra, as well as the enhancement of the particle size and crystallinity, suggest that the activity change observed after heating or drying to powder is due to the formation of surface states which may trap active electrons. This interpretation is also supported by the generated activity of ZnS-100 for the H_2 photoevolution under >350-nm irradiation. ZnS photocatalysis under >350-nm irradiation and relationship with spectroscopic properties are also discussed.

Photoreduction of organic molecules on semiconductor particles has attracted much attention from the viewpoint of solar energy conversion,[2] organic synthesis,[3] and prebiotic chemistry.[4,5] Such irreversible photoreductions, which require at least a net two-electron transfer, have been hitherto carried out by using noble metal deposited semiconductors.[6-8] The deposited metal plays an important role as a relay of conduction band electrons to substrates, being usually believed as a requisite for efficient two-electron reductions on irradiated semiconductors. Cuendet and Grätzel recently disclosed the direct two-electron reduction of pyruvate into lactate under irradiation of aqueous suspensions of nonmetallized TiO_2.[9]

Recent studies on nonmetallized ZnS semiconductor[10-13] revealed that freshly prepared ZnS suspensions are excellent photocatalysts, not only for a water photoreductive H_2 production, but also for phototransformations of various organic substrates such as oxidative carbon–carbon bond formation of organic electron donors and cis–trans photoisomerizations of alkenes. The most notable finding in nonmetallized ZnS photocatalysis is an irreversible two-electron-transfer photoreduction of organic substrates. For example, the ZnS-catalyzed photolysis of primary amines gives secondary amines through photoreduction of Schiff bases formed by photooxidation and condensation of the primary amines,[10d] and the similar photolysis of 2,5-dimethyltetrahydrofuran affords hexane-2,5-diol through photoreduction of 5-hydroxyhexan-2-one which is a primary photooxidation product.[10e]

Another interesting observation is that the photocatalytic activity of ZnS depends strongly on its processing. In fact, recent reports on ZnS samples coprecipitated with another semiconductor or modified with some chemicals revealed the characteristic photocatalysis of ZnS,[14-16] suggesting that processing of ZnS is important for advent of the catalytic activity.

The present report deals with photocatalysis of variously prepared ZnS samples in redox reactions of aldehydes and related compounds in water. Their photocatalytic activities are discussed in terms of their spectroscopic properties. An interesting finding of the work is that surface-state-free aggregation of very small ZnS crystallites catalyzes efficient two-electron-transfer photoreductions of aldehydes and Schiff bases without metal deposition.

(1) Part 7: Yanagida, S.; Miyake, Y.; Midori, Y.; Ishimaru, Y.; Pac, C. *Chem. Express* **1986**, *1*, 399.

(2) (a) Bard, A. J. *J. Phys. Chem.* **1982**, *86*, 172. (b) Grätzel, M. *Energy Resources through Photochemistry and Catalysis*; Academic Press: New York, 1983. (c) Kalyanasundram, K.; Grätzel, M. *Photochem. Photobiol.* **1984**, *40*, 807.

(3) (a) Fox, M. A. *Acc. Chem. Res.* **1983**, *16*, 314. (b) Sakata, T. In *Homogeneous and Heterogeneous Photocatalysis*; Pelizzetti, E., Serpone, N., Eds.; Reidel: Dordrecht, 1986; p 397. (c) Al-Ekabi, H.; de Mayo, P. *J. Org. Chem.* **1987**, *52*, 4756.

(4) Hubbard, J. S.; Hardy, J. P.; Horowitz, N. H. *Proc. Natl. Acad. Sci.* **1971**, *68*, 574.

(5) Dunn, W. W.; Aikawa, Y.; Bard, A. J. *J. Am. Chem. Soc.* **1981**, *103*, 4685.

(6) (a) Nishimoto, S.; Ohotani, B.; Yoshikawa, T.; Kagiya, T. *J. Am. Chem. Soc.* **1983**, *105*, 7180. (b) Yamataka, H.; Seto, N.; Ichihara, J.; Hanafusa, T.; Teratani, S. *J. Chem. Soc., Chem. Commun.* **1985**, 788. (c) Baba, R.; Nakabayashi, S.; Fujishima, A.; Honda, K. *J. Am. Chem. Soc.* **1987**, *109*, 2273. (d) Frank, A. J.; Goren, Z.; Willner, I. *J. Chem. Soc., Chem. Commun.* **1985**, 1029.

(7) Nosaka, Y.; Ishizuka, Y.; Miyama, H. *Ber. Bunsen-Ges. Phys. Chem.* **1986**, *90*, 1199.

(8) Bahnemann, D. W.; Mönig, J.; Chapman, R. *J. Phys. Chem.* **1987**, *91*, 3782.

(9) Cuendet, P.; Grätzel, M. *J. Phys. Chem.* **1987**, *91*, 654.

(10) (a) Yanagida, S.; Azuma, T.; Sakurai, H. *Chem. Lett.* **1982**, 1069. (b) Yanagida, S.; Azuma, T.; Kawakami, H.; Kizumoto, H.; Sakurai, H. *J. Chem. Soc., Chem. Commun.* **1984**, 21. (c) Yanagida, S.; Kawakami, H.; Hashomoto, K.; Sakata, T.; Pac, C.; Sakurai, H. *Chem. Lett.* **1984**, 1449. (d) Yanagida, S.; Kizumoto, H.; Ishimaru, Y.; Pac, C.; Sakurai, H. *Chem. Lett.* **1985**, 141. (e) Yanagida, S.; Azuma, T.; Midori, Y.; Pac, C.; Sakurai, H. *J. Chem. Soc., Perkin Trans. 2* **1985**, 1487. (f) Yanagida, S.; Mizumoto, K.; Pac, C. *J. Am. Chem. Soc.* **1986**, *108*, 647. (g) Yanagida, S.; Miyake, Y.; Midori, Y.; Ishimaru, Y.; Pac, C. *Chem. Express* **1986**, *1*, 399.

(11) Zeug, N.; Bücheler, J.; Kisch, H. *J. Am. Chem. Soc.* **1985**, *107*, 1459.

(12) Reber, J-F.; Meier, K. *J. Phys. Chem.* **1984**, *88*, 5903.

(13) (a) Henglein, A.; Gutiérrez, M. *Ber. Bunsen-Ges. Phys. Chem.* **1983**, *87*, 852. (b) Henglein, A.; Gutiérrez, M.; Fisher, Ch.-H. *Ber. Bunsen-Ges. Phys. Chem.* **1984**, *88*, 170. (c) Weller, H.; Koch, U.; Gutiérrez, M.; Henglein, A. *Ber. Bunsen-Ges. Phys. Chem.* **1984**, *88*, 649.

(14) Kakuta, N.; Park, K.-H.; Finlayson, M. F.; Bard, A. J.; Campion, A.; Fox, M. A.; Weber, S. E.; White, J. M. *J. Phys. Chem.* **1985**, *89*, 732. (b) Kobayashi, J.; Kitaguti, K.; Tsuiki, H.; Ueno, A.; Kotera, Y. *Chem. Lett.* **1985**, 627. (c) Ueno, A.; Kakuta, N.; Park, K. H.; Park, K.-H.; Finlayson, M. F.; Bard, A. J.; Campion, A.; Fox, M. A.; Weber, S. E.; White, J. M. *J. Phys. Chem.* **1985**, *89*, 3828. (d) Kobayashi, J.; Kitaguchi, K.; Tanaka, H.; Tsuiki, H.; Ueno, A. *J. Chem. Soc., Faraday Trans. 1* **1987**, *83*, 1395.

(15) Reber, J-F.; Rusek, M. *J. Phys. Chem.* **1986**, *90*, 824.

(16) Anpo, M.; Matsumoto, A.; Kodama, S. *J. Chem. Soc., Chem. Commun.* **1987**, 1038.

0022-3654/89/2093-2576$01.50/0 © 1989 American Chemical Society

Experimental Section

Materials. Reagent grade acetaldehyde and propionaldehyde from Wako were purified by fractional distillation before use. Extra pure (EP) grade propylamine from Tokyo Kasei was used without further purification. Sodium sulfide, zinc sulfate, ZnS (Nakarai), TiO_2 (Merck), and Pt black were identical with those described in previous papers.[10]

Analyses. Product analysis was carried out by gas chromatography using a Shimadzu GC-7AF apparatus equipped with flame ionization detectors and the following columns: a 0.5 m × 3 mm column of Porapak Q for products from aldehydes; a 0.5 m × 3 mm column of ASC-L for products from propylamine. H_2 evolution was analyzed by GLC using an active carbon column (2 m × 3 mm) on Shimadzu GC-3BT at 100 °C.[10] Paraacetaldehyde and polymeric products (not characterized) from photolysis of acetaldehyde were determined by high-pressure liquid chromatography on TSKgel G2000H 1.2 m × 7.5 mm with a UV detector (Yanagimoto M-315).

UV spectra were recorded on a Hitachi 220A spectrophotometer and ^1H NMR spectra on a JEOL JNM-PMX-60 spectrometer. UV spectra of the ZnS samples were also measured by reflectance spectrophotometry using a Photal (Otsuka Electronics) with a spectro multichannel photodetector (MCPD-100). Steady-state photoluminescence spectra were recorded on a Hitachi 850 spectrometer and luminescence decay curves were measured by using a photon-counting-type nanosecond-time-resolved spectrometer in the instrumental center of Institute for Molecular Science. This consists of a Lambda Physik FL 2002 dye laser pumped by a Lambda Physik 103 MSC excimer laser, a Biomation 6500 transient digitizer, a home-made discriminator, and an NEC 9801 personal computer.

The specific surface area of ZnS powders was determined by the volumetric BET method with a Shimadzu 2205-Ar apparatus using argon as adsorbent. X-ray diffraction was measured with a Rigaku Denki Rota Flex X-ray diffraction apparatus.

ESR spectra of powdered ZnS samples were recorded at room temperature at X band with 100-kHz modulation on a JEOL JS-ME-2X spectrometer. Prior to measurement all samples were thoroughly deoxygenated by the freeze–pump–thaw technique and stored in the dark.

Preparation of ZnS Photocatalysts. ZnS-0 suspensions were prepared in situ under an argon atmosphere by mixing equal amounts of aqueous solutions (0.05 M) of Na_2S and $ZnSO_4$ under magnetic stirring and cooling with ice and water. The pH of the suspensions was adjusted to 7. ZnS-100 suspensions (pH 7) were obtained by refluxing the resulting ZnS-0 suspensions for 10 min on a water bath. Each suspension (25 μmol in 1 mL of water) was used immediately for photoreactions without removing Na_2SO_4. A freshly prepared Na_2S solution is favorable for active ZnS-0 since the solution is easily oxidized by air.[10e]

Powdered ZnS-0 (ZnS-0^P) and powdered ZnS-100 (ZnS-100^P) were prepared in an atmosphere of argon as follows: The ZnS-0 and ZnS-100 were prepared on an ice bath by mixing 500 mL of cold aqueous solutions (0.1 M) of Na_2S and $ZnSO_4$, refluxed for 10 min for ZnS-100 only, and then centrifuged to give their coagulates. They were dried to powder by using a rotary evaporator at room temperature.

Similarly ZnS-0M and ZnS-100M were prepared by using methanolic solutions (0.1 M) and used after drying to powder.

The photocatalyst ZnS-100Zn^P was obtained by drying the similarly refluxed suspension which was prepared from each 500 mL of aqueous $ZnSO_4$ (0.1 M) and Na_2S (0.083 M). For the preparation of ZnS-100S^P, 500 mL of aqueous Na_2S (0.1 M) and the same volume of aqueous $ZnSO_4$ (0.083 M) was used. ZnS-0M–Zn and ZnS-0M–S were prepared similarly as ZnS-0M by using respective methanolic Na_2S (0.083 M) and $ZnSO_4$ (0.1 M) solutions, and $ZnSO_4$ (0.083 M) and Na_2S (0.1 M) solutions, respectively.

General Procedure of ZnS-Catalyzed Photoredox Reactions of Aldehydes. To 1 mL of freshly prepared aqueous ZnS-0 (25 μmol) suspension in a Pyrex tube (8 mm in diameter) was added freshly distilled aldehyde (10 μL, ca. 200 μmol). The resulting solution was flashed with argon gas under cooling on an ice bath, closed with a rubber stopper, and then irradiated with a 300-W high-pressure mercury lamp under cooling with ice and water. Stirring was accomplished by using a magnetic stir bar (5 mm × 2 mm). The generated gas and products were analyzed by GLC.

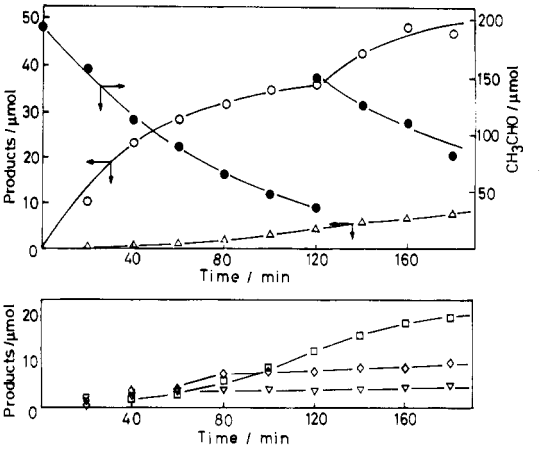

Figure 1. ZnS-catalyzed photoredox reactions of acetaldehyde in water: ○, ethanol; △, H_2; ●, acetaldehyde; □, acetic acid; ▽, biacetyl; ◇, acetoin.

Photoreaction at >350 nm was carried out with an uranyl glass filter.

ZnS-Catalyzed Photoredox Reactions Using Powdered ZnS. All reactions were performed by using 1 mL of an aqueous solution of powdered ZnS (100 mg) and aldehyde (10 μL) as described. The reaction mixture was flashed with argon gas and then irradiated in a similar manner.

ZnS-Catalyzed Photoredox Reactions of Propylamine Using either ZnS-0 or ZnS-100. To a 0.5-mL aqueous ZnS (12.5 μmol) suspension in a Pyrex tube was added 0.5 mL of propylamine (6.1 μmol). The resulting mixture was purged with argon, closed off at atmospheric pressure, and irradiated as described above. The products were confirmed by comparison with authentic samples.

As for the photoreaction using powdered ZnS, 100 mg of ZnS was dispersed in 0.5 mL of water and used as a ZnS suspension. The photoredox reaction with platinized ZnS-0 was undertaken by adding 1.2 mg of platinum black to the ZnS-0 suspension (12.5 μmol).

Photoredox Reactions Using Platinized TiO_2. Anatase TiO_2 was ground with 5 wt % of platinum black. Platinized TiO_2 thus obtained was confirmed to be effective in H_2 photoproduction using methanol as a sacrificial electron donor. An argon-purged suspension of 10 mg of platinized TiO_2 in a mixture of 1.0 mL of distilled water and 10 μL of acetaldehyde was irradiated as described above (Figure 3).

ZnS-Catalyzed H_2 Photoevolution at >350 nm. The reaction mixture of 25 μmol ZnS-0 or ZnS-100, 0.1 mL of triethylamine, and 1 mL of distilled water was flashed with argon gas and irradiated under cooling with ice and water at >350 nm (Figure 11).

Determination of Apparent Quantum Yields. The quantum yields for production of ethanol were determined at 313 nm by using 100 μmol of ZnS-0, 4 mL of distilled water, and 200 μL of acetaldehyde in a 4-mL cuvette cell. The monochromatic light (313 nm) was isolated from a 300-W high-pressure mercury lamp by using an aqueous potassium chromate solution filter (0.2 g/L, 0.1% NaOH). The intensity of incident light was monitored by 2-hexanone actinometry and corrected occasionally with an Eppley thermopile. The quantum yields were calculated by assuming that two photons produce one molecule of ethanol, but were not corrected for light absorption by the suspended catalyst.

Results and Discussion

ZnS-Catalyzed Photoreactions of Acetaldehyde under 313-nm Irradiation. Figure 1 shows the sequence of photoredox reactions of acetaldehyde occurring upon 313-nm irradiation of aqueous ZnS suspensions (ZnS-0) freshly prepared on an ice bath. As

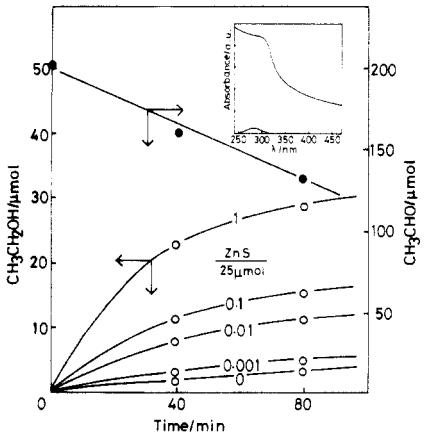

Figure 2. Dependence of ZnS concentration on ethanol photoformation: ○, ethanol formation (Figures are ratios of ZnS-0 to 25 μmol); ●, consumption of acetaldehyde by irradiation in the absence of ZnS-0. The insert is absorption spectra of ZnS-0 and acetaldehyde of the reaction concentration. Spectrum of ZnS-0 was measured by diluting by a factor of 50, and 50 times absorbance was shown for comparison.

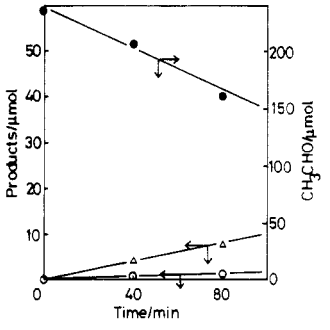

Figure 3. Photoredox reactions of acetaldehyde in water using platinized TiO_2: ○, ethanol; △, H_2; ●, acetaldehyde.

acetaldehyde disappeared, ethanol was produced with acetic acid, diacetyl, acetoin, and a small quantity of H_2 after 80 min irradiation. Evolution of CO_2 (0.05 μmol) and methane (0.6 μmol) was also detected. The products can be classified into photoredox products of acetaldehyde in aqueous medium as shown in Scheme I.

SCHEME I

$$CH_3CHO \xrightarrow[\text{in } H_2O]{\text{ZnS/>290nm}} CH_3CH_2OH + CH_4(\text{trace}) + H_2 + \underset{\text{[photoreduction products]}}{}$$

$$CH_3COOH + CH_3COCOCH_3 + CH_3COCH(OH)CH_3 + \underset{\text{[photooxidation products]}}{}$$

$$CO_2(\text{trace})$$

The apparent quantum yield of ethanol formation was 0.25 at 313 nm. When the aldehyde was added to a photolysate after 120 min irradiation, the rate of ethanol formation was partially restored (ca. 50% of the initial rate). This fact implies that the leveling-off of ethanol formation was partly due to the consumption of the aldehyde.

The material balance based on Figure 1 indicates that after 80 min irradiation, about 50% (60 μmol) of the consumed acetaldehyde should be converted to unidentified products. However, this quantity also corresponds to the consumption of acetaldehyde observed for the photolysis in the absence of ZnS (Figure 2) or in the presence of platinized TiO_2 (Figure 3), suggesting the presence of reactions independent of the ZnS-catalyzed photoredox reaction. In fact, GPC analysis of reaction mixtures detected paraacetaldehyde and unidentified oligomeric products, which were thus disregarded.

Figure 2 shows how the rate of formation of ethanol changes with quantities of ZnS-0 suspension and how negligible the formation of ethanol is in the absence of ZnS-0. These results and the absorption spectra of acetaldehyde and ZnS-0 suspension (the insert in Figure 2) suggest that ZnS-0 should photocatalyze the effective formation of ethanol. As shown in Figure 3, platinized TiO_2 did not catalyze the photoreduction of aldehydes under the comparable conditions; H_2 exclusively evolved with negligible formation of ethanol.

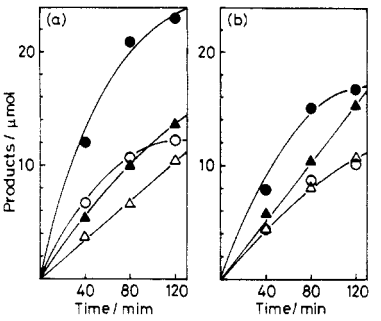

Figure 4. ZnS-catalyzed photoredox reactions of propionaldehyde in water. (a) ○, 1-propanol photoformation catalyzed by ZnS-0; △, H_2 photoevolution catalyzed by ZnS-0; ●, 1-propanol photoformation catalyzed by ZnS-0M; ▲, H_2 photoevolution catalyzed by ZnS-0M. (b) ○, 1-propanol photoformation catalyzed by ZnS-100; △, H_2 photoevolution catalyzed by ZnS-100; ●, 1-propanol photoformation catalyzed by ZnS-100M; ▲, H_2 photoevolution catalyzed by ZnS-100M.

Photoreductions with Powdered ZnS or with Heat-Treated ZnS Suspensions. It has now been found that the photocatalytic activity of ZnS depends on preparation conditions, especially on preparation temperature. The ZnS suspension (ZnS-100) obtained by refluxing the ZnS-0 suspension for 10 min showed a decrease in photocatalytic activity (ca. one-half) for the formation of ethanol, whereas the activity for the H_2 production was increased by a factor of ca. 3. Comparison of the ZnS-0 suspension with ZnS-100 suspension was extended to photoreduction of propionaldehyde. As shown in Figure 4, the photoreduction of propionaldehyde again gave 1-propanol but was accompanied by a more competitive H_2 production than that of acetaldehyde. With ZnS-100, the formation of 1-propanol was slightly decreased.

The photoreduction was also carried out using some powdered ZnS catalysts. Active ZnS powder (ZnS-OM) was prepared by drying the suspension obtained from cold methanolic solutions of $ZnSO_4$ and Na_2S. The effect of heat treatment was also examined by using the ZnS powder (ZnS-100M) obtained from the refluxed methanolic ZnS-0. When ZnS-0M or ZnS-100M powder (see Experimental Section) was used in the photolysis of propionaldehyde, the more efficient photoreduction could be observed. With ZnS-0M, 1-propanol was formed more efficiently than H_2 (Figure 4a), and the refluxing effect already observed with ZnS-100 could be confirmed for ZnS-100M (Figure 4b).

On the other hand, some commercially available ZnS powder was found to be active only for H_2 production in the photolysis of propionaldehyde but Nakarai's ZnS showed only weak activities for both the 1-propanol photoproduction (0.5 μmol/h) and the H_2 photoevolution (1.4 μmol/h) (see Table II).

ZnS-Catalyzed Photoconversion of Propylamine to Dipropylamine. In our preceding paper,[10d] the ZnS-catalyzed photolysis of ethylamine in water was established to give diethylamine with the formation of a small amount of H_2. This conversion was interpreted as due to the photoreduction of *N*-ethylidenethylamine formed by the condensation of ethylamine with acetaldehyde formed by hydrolysis of the primary oxidation product as shown by eq 2 and 3 in Scheme II.

SCHEME II

$$ZnS \xrightarrow{313nm} e_{CB} + h_{VB} \quad (1)$$

$$RCH_2NH_3 \xrightarrow[-2H^+]{2h_{VB}} RCH{=}NH \xrightarrow[-NH_3]{H_2O} RCHO \xrightarrow[-H_2O]{RCH_2NH_2} RCH{=}NCH_2R \quad (2)$$

$$RCH{=}NCH_2R \xrightarrow{2e_{CB},2H^+} (RCH_2)_2NH \quad (3)$$

The photolysis of propylamine in the presence of ZnZ-0 or ZnS-100 suspensions reveals remarkable differences in activities

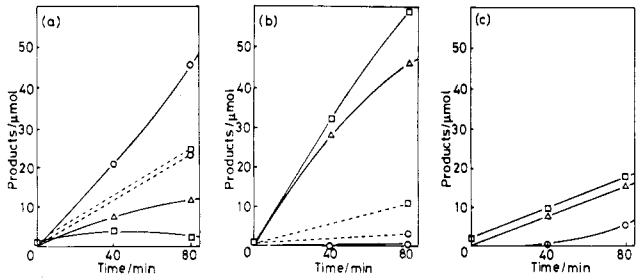

Figure 5. ZnS-catalyzed photoredox reactions of propylamine in water: O, dipropylamine; △, *N*-propylidenepropylamine; □, H_2; (a) solid line, catalyzed by ZnS-0, and dotted line, catalyzed by ZnS-0^P; (b) solid line, catalyzed by ZnS-100, and dotted line, catalyzed by ZnS-100^P; (c) solid line, catalyzed by ZnS-0 with platinum black.

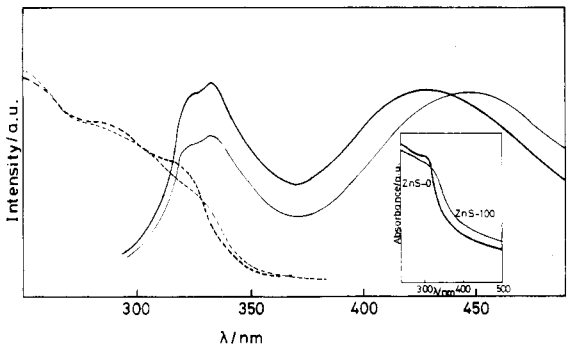

Figure 6. Photoluminescence spectra of ZnS-0 (bold line) and ZnS-100 (fine line) excited at 260 nm and their excitation spectra (corresponding dotted lines) monitored at 450 nm. ZnS (diatomic) concentration is 2.5 × 10^{-4} M. Insert: their absorption spectra at the same concentration.

as shown in Figure 5. The former was very efficient for the conversion to dipropylamine while the latter was much more efficient for H_2 production with the accumulation of *N*-propylidenepropylamine without undergoing photoreduction to dipropylamine. When ZnS-0 and ZnS-100 suspensions were dried to the powder (ZnS-0^P and ZnS-100^P), the former showed a decrease in selectivity to dipropylamine and the latter a decrease in activity as shown in Figure 5, a and b. On the other hand, the photolysis with ZnS-0 suspension combined with platinum black showed decreases in both activity and selectivity as shown in Figure 5c.[17]

Comparison of Spectroscopic Properties of ZnS-0 and ZnS-100 Suspensions. The insert in Figure 6 shows UV absorption spectra of ZnS-0 and ZnS-100 suspensions which were measured after diluting to a hundredth of the suspensions used for photolysis. The absorption spectrum of ZnS-0 suspension is comparable with that observed by Brus and his group.[18] The spectrum of ZnS-100 is shifted slightly to a longer wavelength, suggesting the growth of particle size.[19]

Figure 6 shows their photoluminescence spectra excited at 260 nm and their excitation spectra monitored at 450 nm. Both suspensions show three emission maxima when measured without being exposed to excitation light.[20] The shorter wavelength emissions with peaks at 323 and 334 nm occur close to the band gap wavelength of 339 nm (3.66 eV). Although the origin of two peaks of the emission band is not clear at present, they may be assigned to the band gap emission, since they almost coincide with the first maximum of the excitation spectra. To our knowledge, this is the first observation of the band gap emission of ZnS. However, careful examination of Figure 6 reveals that the emission starts almost from 300 nm. This is much shorter than the band gap of ZnS and coincides with the plateau edge in the ZnS-0 absorption spectrum (insert). This fact strongly suggests that the present ZnS-0 and ZnS-100 contain very fine particles whose emission is near 300 nm because of size quantization effects.[21,22]

TABLE I: Analysis of Emission Decay of ZnS-0 and ZnS-100 Suspensions

ZnS	τ/ns (ratio) decay at 350 nm[a]	τ/ns (ratio) decay at 430 nm[b]
ZnS-0	15 (0.67)	6 (0.69)
	34 (0.33)	14 (0.24)
		55 (0.064)
		500 (0.006)
ZnS-100	10 (0.70)	6 (0.68)
	28 (0.30)	15 (0.27)
		66 (0.0044)
		550 (0.0044)

[a] Assuming two components as follows: $I(t) = I_1(0)e^{-t/\tau_1} + I_2(0)e^{-t/\tau_2}$. [b] Assuming four components as follows: $I(t) = I_1(0)e^{-t/\tau_1} + I_2(0)e^{-t/\tau_2} + I_3(0)e^{-t/\tau_3} + I_4(0)e^{-t/\tau_4}$.

The longer wavelength emission was assigned to the emission from self-activated sites (SA) which result from defect sites such as vacancies in lattice or interstitial impurities.[13c,23] In other words, the SA emission indicates the presence of localized states in both suspensions. However, their maxima are slightly different from each other and the maximum of the ZnS-100 emission shifts toward longer wavelength, supporting the growth of particle size as the cause of the shift observed in the excitation spectrum of ZnS-100.[13c]

On careful examination of the excitation spectra, the spectrum of ZnS-0 shows not only the shift to the shorter wavelength but also the broad but clear structure. The maximum around 280 nm closely coincides with the reported maximum of the quantum size exciton peak of ZnS.[18]

These spectroscopic observations suggest that both suspensions (ZnS-0 and ZnS-100) should consist of very small ZnS crystallites and their loose aggregation. The microcrystallites should increase in size on heating as seen in the case of ZnS-100.

Figure 7a–c shows the time-resolved decay curve of the band gap and SA emissions observed for ZnS-0 and ZnS-100 suspensions. The band gap emission is fitted well by two exponentials in both ZnS-0 and ZnS-100 as the solid lines represent. The lifetime of the faster decay component is 15 ns for ZnS-0 and 10 ns for ZnS-100, indicating that the thermal treatment at 100 °C brings a decrease in the lifetime of the band gap emission. This result is important from the viewpoint of photocatalysis, because the longer lifetime of active electrons in the conduction band is advantageous to the photocatalytic reduction. This result coincides well with difference in the photocatalytic activity between ZnS-0 and ZnS-100. On the other hand, the decay curves of the SA emission were almost the same for both suspensions, and the convolution analysis indicates that they are well reproduced by using four exponentials as shown in Table I.

Physical Properties of Powdered ZnS-0 and ZnS-100. Since ZnS-0^P and ZnS-100^P retain the difference in photocatalytic activity, their spectroscopic and physical properties were compared to establish the relationship between powder structure and activity. The specific surface area was determined to be 94 m^2/g for ZnS-0^P and 96 m^2/g for ZnS-100^P. Both powder X-ray diffraction spectra showed broad patterns supporting sphalerite (cubic) structure and the slightly sharper spctrum of ZnS-100^P reflected a slight increase in size and/or crystallinity by heat treatment.[19]

(17) The similar platinum effect could be confirmed for the photoreaction of acetaldehyde; the photoreduction to ethanol was retarded and the H_2 evolution was increased.

(18) Rossetti, R.; Hull, R.; Gibson, J. M.; Brus, L. E. *J. Chem. Phys.* **1985**, *82*, 552.

(19) (a) Sidot, T. *Compt. Rend.* **1866**, *62*, 999. (b) Dafinova, R.; Kynev, K. *Z. Naturforsch.* **1981**, *36a*, 1391.

(20) Henglein and his group reported that the ZnS suspension stabilized by colloidal SiO_2 showed only the SA fluorescence.[13a] Reinvestigation revealed that both fluorescence peaks are initially present under the similar conditions but, upon exposure to the excitation light, the SA fluorescence increases with increasing time of irradiation. Details will be reported elsewhere.

(21) (a) Rossetti, R.; Nakahara, S.; Brus, L. E. *J. Chem. Phys.* **1983**, *79*, 1086. (b) Brus, L. E. *J. Chem. Phys.* **1983**, *79*, 5566. (c) Rossetti, R.; Ellison, J. L.; Gibson, J. M.; Brus, L. E. *J. Chem. Phys.* **1984**, *80*, 4464. (d) Brus L. E. *J. Chem. Phys.* **1984**, *80*, 4403. (e) Brus, L. E. *J. Phys. Chem.* **1986**, *90*, 2555.

(22) Chestnoy, N.; Hull, R.; Brus, L. E. *J. Chem. Phys.* **1986**, *85*, 2237.

(23) Becker, W. G.; Bard, A. J. *J. Phys. Chem.* **1983**, *87*, 4888.

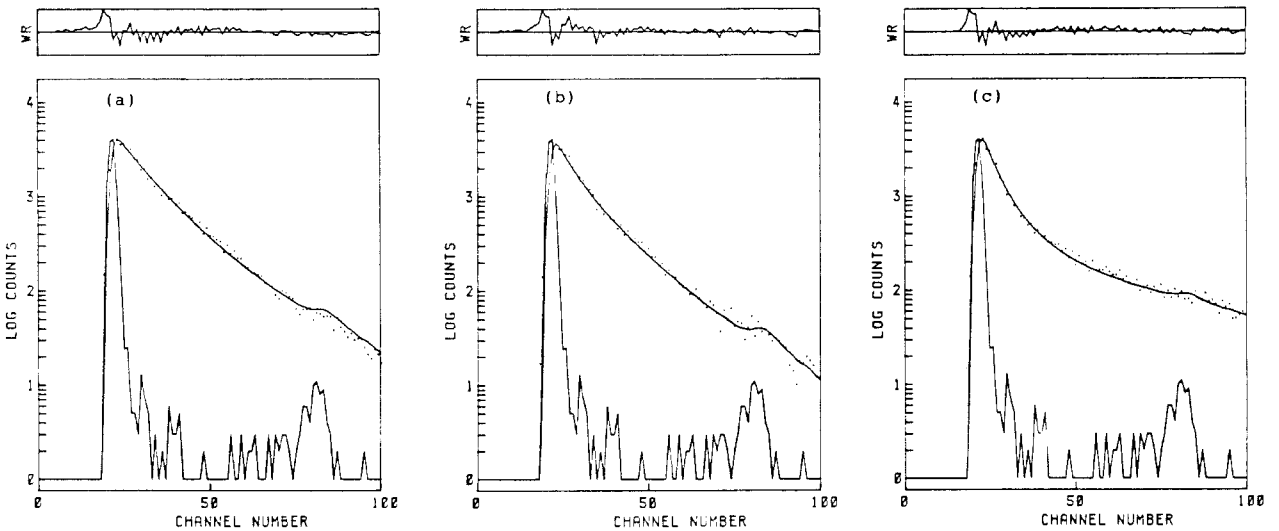

Figure 7. Photoluminescence decay curves of ZnS suspensions: (a) ZnS-0 at 350 nm excited at 308 nm; (b) ZnS-100 at 350 nm excited at 308 nm; (c) ZnS-0 at 430 nm excited at 308 nm (almost identical with that of ZnS-100 observed under the same conditions (see Table I).

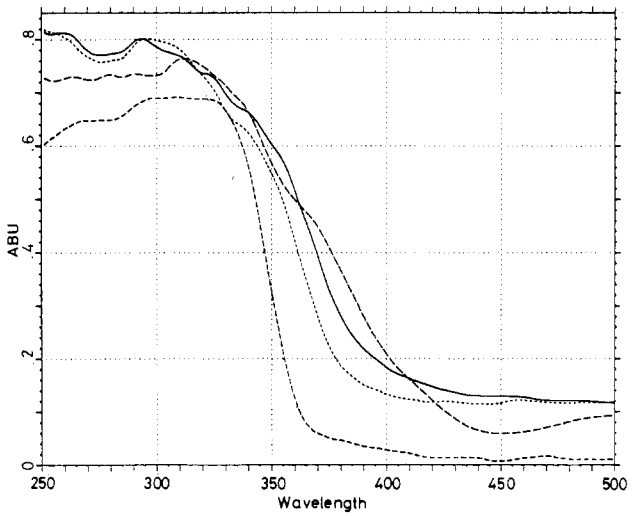

Figure 8. Absorption spectra of ZnS photocatalysts by reflectance spectrophotometry using a Photal: —, ZnS-100^P;···, ZnS-0^P; - - -, ZnS-0 coagulate;– – –, Nakarai ZnS.

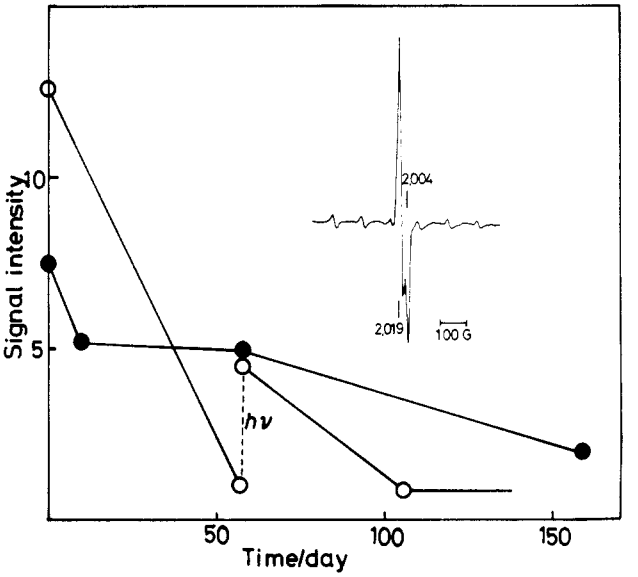

Figure 9. Time–signal intensity plots for ESR signals of ZnS-0^P and ZnS-100^P: ○, ZnS-0^P; ●, ZnS-100^P. The signal intensity was obtained as a ratio to signals due to the included Mn^{2+} in ZnS-0^P and ZnS-100^P. The insert is the ESR spectrum of ZnS-0^P observed at room temperature. The small signals are due to Mn^{2+}.

Figure 8 shows the reflectance spectra of ZnS-0^P, ZnS-100^P, Nakarai ZnS, and the wet ZnS-0 coagulate obtained by centrifugation of ZnS-0 suspension. ZnS-0^P shows a more blue-shifted onset of spectrum than ZnS-100^P as observed for the UV absorption and excitation spectra of their diluted suspensions. Compared with both absorption spectra of ZnS-0^P and ZnS-100^P, the wet ZnS-0 coagulate is characterized by the steep absorption threshold and the onset blue-shifted as much as 27 nm, whereas the plateau edge is consistent with the band gap absorption. On the other hand, Nakarai ZnS shows a gently sloping spectrum with the same plateau edge but with the most red-shifted onset.

Both ZnS-0^P and ZnS-100^P reveal ESR signals in the dark without UV irradiation as shown in the insert of Figure 9, assignable to trapped electrons (F color center).[10f] Interestingly, on standing under dark at room temperature, their signals change differently in intensity and the intensity is increased on UV irradiation and again decreased under dark as shown in Figure 9. These observations imply that the electron produced during the workup[16,24] or by the photoexcitation should be readily trapped on the localized states of ZnS crystallites and their situation should be different between ZnS-0^P and ZnS-100^P.

Photocatalysis under >350-nm Irradiation. We previously reported that photoexcitation of ZnS to active surface states by >350-nm irradiation leads to H_2 production in the presence of

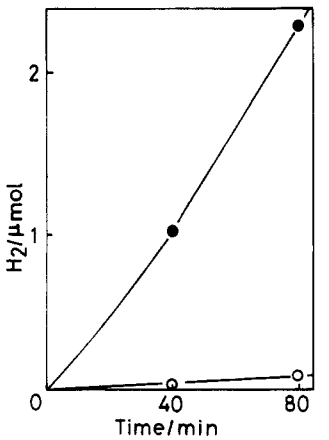

Figure 10. Photocatalysis of triethylamine by ZnS-0 and ZnS-100. H_2 photoevolution under >350-nm irradiation. ●, ZnS-100; ○, ZnS-0. See Experimental Section.

appropriate sacrificial electron donors.[10g] Figure 10 shows H_2 production in the photolysis of triethylamine in the presence of ZnS-0 or ZnS-100 under >350-nm irradiation. It has been found

(24) Schneider, J.; Räuber, A. *Solid State Commun.* **1967**, *5*, 779.

TABLE II: ZnS-Catalyzed Photoreductions of Propionaldehyde in Water under >350-nm or 313-nm Irradiation

ZnS	wavelength/nm	induction[a]	rate/(μmol/h)[b] 1-propanol	H_2
ZnS-0	313	no	12.9	5.2
	>350	short	0	trace
ZnS-100	313	no	6.5	6.0
	>350	short	1.2	0.1
ZnS-100Zn^p	313	short	0.7	0.2
	>350	short	1.4	0.4
ZnS-100S^p	313	long	0.3	0.1
ZnS-0M-Zn	313	no	3.4	1.7
	>350	short	2.4	0.2
ZnS-0M-S	313	long	1.9	0.5
ZnS (Nakarai)	313	no	1.4	0.5
	>350	long	0.9	0.3

[a] Judged from the plot vs irradiation time. [b] Initial rates were obtained for the noninduction reactions, and maximum rates obtained for other reactions.

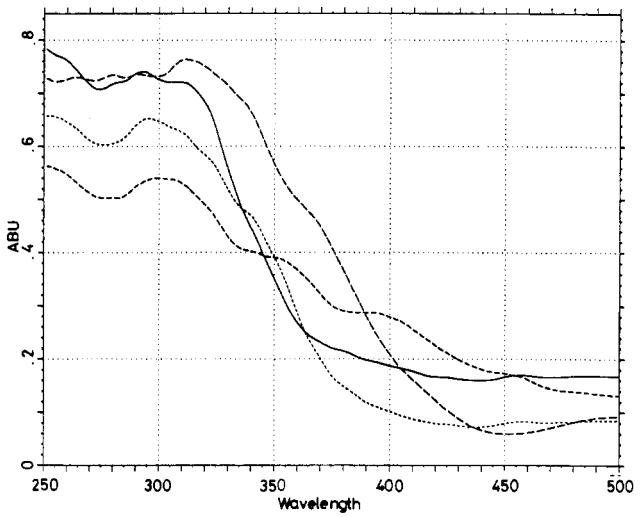

Figure 11. Absorption spectra of powdered ZnS photocatalysts by reflectance spectrophotometry using a Photal: —, ZnS-0M-Zn; ···, ZnS-100Zn^p; - - -, ZnS-100S^p; – – –, Nakarai ZnS.

that ZnS-100 has an activity for H_2 evolution under UV light which is lower than the intrinsic band gap energy.

ZnS-catalyzed photolysis under >350-nm irradiation was extended to photoreduction of propionaldehyde (Table II), because some electrons excited directly to the surface states of ZnS under the irradiation should have a potential to reduce aldehydes to alcohols. The ZnS powders which contain excess of either Zn^{2+} or S^{2-} (ZnS-100Zn^p, ZnS-100S^p, and ZnS-0M-Zn) were prepared by using 20% excess of either $ZnSO_4$ or Na_2S solutions. ZnS powder prepared with excess of S^{2-} showed poor photocatalytic activity under 313-nm irradiation, and ZnS-0M-Zn prepared in methanol by using 20% excess of Zn^{2+} was found rather effective for the photoreduction of propionaldehyde to 1-propanol under >350-nm irradiation. In general, photoreactions under >350-nm irradiation are not only inefficient but also are accompanied by induction periods when compared with those under 313-nm irradiation. Induction periods may be related with the creation of catalytic sites.

Figure 11 shows the reflectance spectra of ZnS-0M-Zn, ZnS-100Zn^p, ZnS-100S^p, and Nakarai ZnS which were all used for the photolysis under >350-nm irradiation. Compared with Figure 8, the ZnS obtained in the presence of excess Zn^{2+} show gently sloping reflectance spectra with shoulder peaks. Further, as shown in Figure 12, ZnS-0M-Zn showed the strongest emission with maximum around 420 nm, while those obtained in the presence of excess S^{2-} show complex reflectance spectrum, and the fluorescence was negligible as illustrated in Figure 12. The observation suggests that excess of Zn^{2+} should create surface states through the formation of sulfur vacancy on the ZnS

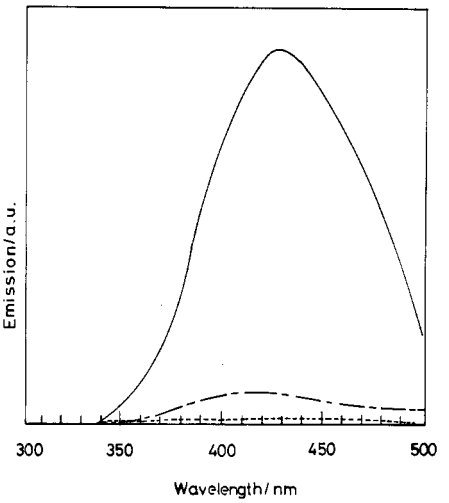

Figure 12. Photoluminescence spectra of ZnS photocatalysts prepared by using methanolic solutions: —, ZnS-0M-Zn; -·-, ZnS-0M; - - -, ZnS-0S^p.

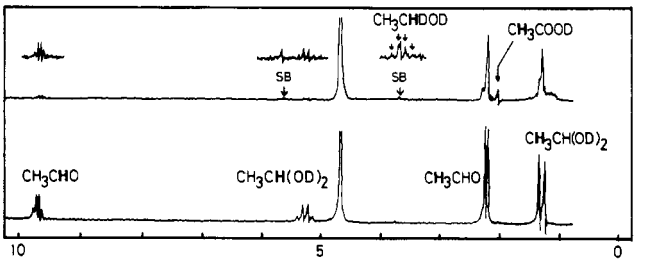

Figure 13. ^1H NMR spectra of a mixture of D_2O, acetaldehyde, and ZnS-0 prepared by using D_2O before (bottom) and after (top) irradiation at >290 nm.

crystallites and they should work as electron-trapping sites which serve as catalytic sites for photoreductions under >350-nm irradiation.

Mechanism. The observed photoredox reactions of acetaldehyde on ZnS-0 can be explained by eq 1 in Scheme II and eq 4–9 of Scheme III.

SCHEME III

$$CH_3CHO \underset{h_{VB},-H^+}{\overset{e_{CB},H^+}{\rightleftharpoons}} \underset{\mathbf{1}}{CH_3\dot{C}HOC} \xrightarrow{e_{CB},H^+} CH_3CH_2OH \quad (4)$$

$$CH_3CHO \underset{e_{CB},H^+}{\overset{h_{VB},-H^+}{\rightleftharpoons}} \underset{\mathbf{2}}{CH_3\dot{C}{=}O} \xrightarrow{h_{VB},OH^-} CH_3COOH \quad (5)$$

$$\mathbf{1} + \mathbf{2} \rightarrow \underset{\mathbf{3}}{CH_3COCH(OH)CH_3} \quad (6)$$

$$\mathbf{2} + \mathbf{2} \rightarrow \underset{\mathbf{4}}{CH_3COCOCH_3} \quad (7)$$

$$\mathbf{3} \xrightarrow{2h_{VB},-2H^+} \mathbf{4} \quad (8)$$

$$\mathbf{4} \xrightarrow{2e_{CB},2H^+} \mathbf{3} \quad (9)$$

$$\mathbf{1} + \mathbf{1} \rightarrow CH_3CH_2OH + CH_3CHO \quad (10)$$

Figure 13 shows ^1H NMR spectra monitored before and after irradiation of a mixture of acetaldehyde and ZnS-0 suspension in D_2O. The spectrum before irradiation clearly indicates that acetaldehyde is equilibrated with the hemiacetal.[25] An interesting observation is that irradiation resulted in the rapid coalescence of the two doublets of the methyl protons of both acetaldehyde and the hemiacetal into singlets. In addition, the coalescence is accompanied by decreases in relative intensities of the signals of both CH_3CHO and $CH_3CH(OH)_2$ and the water signal increased.

(25) Rocek, J. In *The Chemistry of the Carbonyl Group*; Patai, S., Ed.; Interscience: New York, 1966; p 467.

These facts strongly indicate that a rapid H–D exchange occurs at the α-carbon of the aldehyde under irradiation and that the one-electron-transfer photoredox reactions of acetaldehyde should reversibly occur on irradiated ZnS-0 as shown in eq 4 and 5. In the TiO_2/Pt system, such H–D exchange reactions were not observed.

According to the interfacial energy scheme at the (ZnS/electrolyte) interface at pH 1, the conduction band edge, E_c, was reported to be −1.74 V vs SCE.[26] Considering the negative shift of about 55 mV per pH unit increment, E_c at pH 7 is negative (−2.07 V vs SCE) enough to well explain the smooth photoreduction of acetaldehyde ($E_{1/2}$ = −1.65 V vs SCE)[27] to ethanol by electrons on the conduction band (e_{CB}). Suppression of electron transfer to H^+ on ZnS-0 suspension may be rationalized as due to inverted region effects,[28] i.e., a large energy change as much as 2 eV for e_{CB} transfer to H^+. On the other hand, the formation of surface states should become profitable for H_2 evolution due to the decreased energy change in electron transfer from trapped sites. The valence band (1.59 V vs SCE) is positive enough to oxidize acetaldehyde whose E_p(Pt/$HClO_4$, 1 M) is reported to be 0.75–1.00 V vs SCE.[29]

The following facts also support a sequential transfer of e_{CB} on irradiated ZnS-0. (a) The 350-nm emission observed for ZnS-0 has the longest lifetime, indicating the presence of long-lived active electrons (e_{CB}). (b) Active ZnS-0 has the blue-shifted UV and excitation spectra with the steep onset, indicating fewer surface states where active electrons might migrate. (c) Disproportionation of hydroxyethyl radical (**1**) shown in eq 10 of Scheme III seems to be inadequate as an alternative mechanism for the reduction to alcohol, because the formation of acetoin (eq 6) was observed only at the beginning of photolysis, and butane-2,3-diol, a coupling product of **1**, could not be detected.[30]

Influence of heat treatment, drying to powder, and added Pt black on the two-electron-transfer catalysis can be rationalized as due to the formation of localized energy levels, i.e., surface states in the forbidden zone of ZnS particles. The observation of gentle-sloping and red-shifted onsets of UV spectra and SA emissions are strong evidence for the formation of localized states. Such localized states should act favorably at surface as catalytic sites for the H_2 photoproduction.

The photocatalysis of ZnS-100^P under >350-nm irradiation also supports the presence of surface states in the forbidden zone. The localized states which give rise to a strong SA emission should be responsible for photocatalysis under >350-nm irradiation as reported in the previous paper.[10g] The enhanced activity at >350 nm when prepared with excess Zn^{2+} is also attributable to the formation of such active surface states as in the cases of ZnS-100Zn^P and ZnS-0M–Zn. Pt black may also give rise to a surface state as a trapping site for electrons, leading to the decreased activity for the photoreduction to ethanol.

Recently, size quantization effects that arise from the confinement of charge carriers in small semiconductor particles are under active investigation[18,21,22] and have been focused on photocatalytic activities.[31–34] At first glance, the loose structure of the ZnS suspensions seemed to suggest quantization effects on the direct photoreductions. However, the spectroscopic properties supporting the presence of quantized ZnS particles was obtained when the reaction suspension was diluted to the order of 10^{-4} M. Further, very small ZnS crystallites have a tendency to grow up to their extensive aggregation especially at higher concentration and the rate of photoreduction increases with a increasing ZnS diatomic concentration (Figure 2). These observations and the consistent energetics between reactants and ZnS suggest that quantized ZnS particles should contribute at least to construction of their aggregation which is free from localized states. Further investigation is in progress for the elucidation of the contribution of size quantization effects on sequential two-electron-transfer photoreductions on irradiated semiconductors.

Conclusion

It is important from a point of view of semiconductor photocatalysis that photoexcited electron on freshly prepared ZnS suspension migrate efficiently to aldehydes and related compounds without any electron relay, showing sequential two-electron-transfer reductions. Such ZnS suspension consists of aggregation of very small crystallites and is free from the surface states which result from defect sites. Processing such as reflux and drying is accompanied by change of particle size or crystallinity and results in the formation of surface states. The surface states play a decisive role in catalytic activities of the processed ZnS. Utilization of active surface states leads to ZnS photocatalysis under the irradiation of light lower than the intrinsic band gap energy.

The present photoreaction of aliphatic aldehydes is a photoinduced disproportionation of the aldehydes and may be called "photo-Cannizzaro reaction of aliphatic aldehydes", since the Cannizzaro reaction of aliphatic aldehydes is generally impossible because of the ease of their aldol condensation in the presence of alkali.

Acknowledgment. This work was supported by Joint Studies Program (1984–1985) of the Institute for Molecular Science, by the Iwatani Naoji Foundation's Research Grant, and by a Grant-in-aid for Scientific Research from the Ministry of Education, Science and Culture, Japan (Nos. 61550617 and 62213021).

Registry No. ZnS, 1314-98-3; CH_3CHO, 75-07-0; CH_3CH_2CHO, 123-38-6; CH_3CH_2OH, 64-17-5; CH_3CO_2H, 64-19-7; $CH_3COCOCH_3$, 431-03-8; $CH_3COCH(OH)CH_3$, 513-86-0; H_2, 1333-74-0; CO_2, 124-38-9; CH_4, 74-82-8; $CH_3CH_2CH_2OH$, 71-23-8; $CH_3CH_2CH_2NH_2$, 107-10-8; $(CH_3CH_2CH_2)_2NH$, 142-84-7; $CH_3CH_2CH{=}NCH_2CH_2CH_3$, 7707-70-2; triethylamine, 121-44-8.

(26) Fan, F.-R. F.; Leempoel, P.; Bard, A. J. *J. Electrochem. Soc.* **1983**, *130*, 1866.
(27) *CRC Handbook Series in Organic Electrochemistry*; Meites, L., Zuman, F., Eds.; CRC Press: Cleveland, OH, 1976; p 30.
(28) Miller, J. R. *Nouv. J. Chem.* **1987**, *11*, 83 and references cited therein.
(29) Kutsuchker, A.; Vielstich, W. *Electrochim. Acta* **1963**, *8*, 985.
(30) Although it was indeed formed from **1** produced by a ZnS-photocatalyzed oxidation of ethanol (unpublished results).
(31) (a) Nozik, A. J.; Williams, F.; Nenadović, M. T.; Rajh, T.; Micić, O. I. *J. Phys. Chem.* **1985**, *89*, 397. (b) Nozik, A. J.; Thacker, B. R.; Turner, J. A.; Olson, J. M. *J. Am. Chem. Soc.* **1985**, *107*, 7805. (c) Nedeljković, J. M.; Nenadović, M. T.; Micić, D. I.; Nozik, A. J. *J. Phys. Chem.* **1986**, *90*, 12.
(32) Bahnemann, D. W.; Kormann, C.; Hoffmann, M. R. *J. Phys. Chem.* **1987**, *91*, 3789.
(33) (a) Koch, U.; Fojtik, A.; Weller, H.; Henglein, A. *Chem. Phys. Lett.* **1985**, *122*, 507. (b) Spanhel, L.; Haase, M.; Weller, H.; Henglein, A. *J. Am. Chem. Soc.* **1987**, *109*, 5649.
(34) (a) Anpo, M.; Shima, T. *Chem. Express* **1987**, *2*, 193. (b) Anpo, M.; Shima, T.; Kodama, S.; Kubokawa, Y. *J. Phys. Chem.* **1987**, *91*, 4305.